炭素 TANSO
2019 [No.286] 9-13

Preparation and characterization of activated carbons produced from oil palm empty fruit bunches

Tomoyoshi Sakamoto[a)], Muhammad Abbas Ahmad Zaini[b),c)], Yoshimasa Amano[d),e)] and Motoi Machida[d),e),*]

Activated carbons were prepared by activating oil palm empty fruit bunches (EFB) using various chemicals including H_3PO_4, KOH or $ZnCl_2$ and were characterized by elemental analysis, nitrogen and methylene blue adsorption. The effect of the pre-treatment of EFB by NaOH was also investigated. Among all samples, EFB pre-washed with NaOH and then activated with $ZnCl_2$ showed the greatest maximum adsorption capacity (357 mg/g) and BET specific surface area (1265 m^2/g). The experimental data of all adsorbents were well fitted to the Langmuir isotherm model and pseudo-second-order kinetics model. This study demonstrated that $ZnCl_2$ activation was the best way to obtain an activated carbon, and that NaOH pre-washing was effective as well for developing mesopores in EFB activated by H_3PO_4 and $ZnCl_2$.

KEYWORDS : Empty fruit bunches, Activated carbon, Methylene blue

1. Introduction

Palm oil ranks first among the vegetable oil and fat manufactures and has been mainly produced in Southeast Asia. In 2017, 67 million tons of palm oil was produced all over the world and 21 million tons of which was in Malaysia[1)]. Generally, palm oil has been included in various processed foods due to containing the great value of palmitic acid content which prevents the oil from oxidation[2)]. In addition, there are diverse usability for palm oil; cooking oil, detergent, candle, cosmetics and fuel.

A great amount of residual wastes, such as empty fruit bunches (EFB), coconut shell, palm leaves and palm stems, was also produced together with palm oil. Recently, several researches and developments activities have suggested the reuse and recycle of palm oil waste[3)]. Especially, the palm oil manufacture process disposes approximately 1.1 tons of EFB in every ton of palm oil production[4)], therefore, in Malaysia, 23 million tons of EFB was produced in 2017 alone. The EFB is presently utilized to generate electricity at thermal power stations and reshaped as fuel pellet to substitute coal cokes at coal-fired power plants. The mass production of fuel pellet made from EFB has already been in operation since 2011, as manifestation of Malaysian government policy of "National Biomass Strategy" . The power plants and manufacturing factories are increasing year by year[5)]. Similarly, other studies have suggested that EFB has the potential to be used as high density fiber boards[6)], alternative substrates[7)] and activated carbons. Notably, activated carbons have been focused on owing to their large adsorption capacity, high surface area, low cost and easy regeneration. In the previous research, the EFB-based activated carbons were prepared by KOH activation for methylene blue[8)] and H_2 gas adsorption[9)], and by CO_2 activation[10)] for urea adsorption[11)]. Although H_3PO_4 and $ZnCl_2$ are generally used to prepare activated carbon, there are few researches on investigating on the effectiveness and comparison among H_3PO_4, KOH and $ZnCl_2$ activation for EFB so as to evaluate the methylene blue adsorption capacities by the derived activated carbons.

In this study, EFB was activated by H_3PO_4, KOH or $ZnCl_2$ for the comparison of their methylene blue (MB) adsorption capacities. On the other hand, it has been proposed that alkaline pre-washing treatment of precursor before chemical activation could lead to the development of pore structures[12)]. Thus, EFB was also treated by NaOH and then activated by the same chemical activators in order to enhance the methylene blue adsorption. It is expected that this study could provide much support for the reuse of EFB as activated carbon, other than fuel.

* Corresponding Author, E-mail: machida@faculty.chiba-u.jp
(Received March 27, 2018, Accepted November 19, 2018)
a) Graduate School of Science and Engineering, Chiba University: 1-33 Yayoi-cho, Inage-ku, Chiba 263-8522, Japan
b) Centre of Lipids Engineering & Applied Research, Ibnu-Sina Institute for Scientific & Industrial Research, Universiti Teknologi Malaysia: 81310 UTM Johor Bahru, Johor, Malaysia
c) School of Chemical & Energy Engineering, Faculty of Engineering, Universiti Teknologi Malaysia: 81310 UTM Johor Bahru, Johor, Malaysia
d) Graduate School of Engineering, Chiba University: 1-33 Yayoi-cho, Inage-ku, Chiba 263-8522, Japan
e) Safety and Health Organization, Chiba University: 1-33 Yayoi-cho, Inage-ku, Chiba 263-8522, Japan
http://dx.doi.org/10.7209/tanso.2019.9

2. Materials and Methods

The natural empty fruit bunches (EFB) was supplied by Adela palm oil mill factory located in Kota Tinggi, Johor, Malaysia. The raw-EFB was dried in an oven at 105 °C for 24 h. Approximately 15 g of the dried-EFB was impregnated in 300 mL of H_3PO_4 (0.51 mol/L), KOH (0.89 mol/L) or $ZnCl_2$ (0.37 mol/L) solution at the same weight ratio (chemical activator to EFB) of 1.0 for 3 h with stirring in a beaker at room temperature. After drying in an oven at 105 °C for 24 h, the sample was transferred to a crucible and covered by aluminum foil, and then heated at 600 °C for 1 h using furnace in ambient atmosphere. These EFB samples activated by H_3PO_4, KOH and $ZnCl_2$ were designated as P, K and Z, respectively. After that, the activated EFB was soaked into 1.0 mol/L HCl for 24 h and washed with hot distilled water for 6 h using Soxhlet extractor to remove excess chemical before drying in an oven at 105 °C for 24 h. As a control, the EFB carbonized at 600 °C for 1 h (without activation process) was also prepared and named as C.

Approximately 10 g of the dried EFB was added into NaOH solution (10 g of NaOH solid was dissolved in 300 mL distilled water) in a beaker. The solution was stirred for 3 h at room temperature. The sample was washed with distilled water several times and soaked into 1 mol/L HCl for 24 h. After drying in an oven at 105 °C for 24 h, the sample was activated using the same procedures as previously mentioned. The NaOH pretreatment activated by H_3PO_4, KOH and $ZnCl_2$ was referred to as NP, NK and NZ, respectively. The EFB pretreated by NaOH and carbonized at 600 °C for 1 h (without activation process) was prepared as well, and named as NC.

In order to investigate the adsorbent properties, the Langmuir adsorption isotherm, adsorption kinetics, the BET specific surface area, pore structures and the elemental composition were evaluated. For adsorption isotherm experiment, approximately 30 mg of ground adsorbent and 15 mL MB solution of different concentrations (25 ~ 300 mg/L for C and NC; 50 ~ 500 mg/L for P and K; 50 ~ 1000 mg/L for Z, NP, NK and NZ) were added into a glass bottle and capped. All bottles were left at room temperature for 24 h under static condition. The concentration of MB solution was measured at a wavelength of 570 nm using DU-8200 UV/Vis spectrophotometer (Shanghai Drawell Scientific Instrument Co., Ltd., China). The maximum adsorption amount, Q_m [mg/g], was calculated by Eq. (1):

$$\frac{C_e}{Q_e} = \frac{C_e}{Q_m} + \frac{1}{Q_m K_e} \quad \cdots\cdots (1)$$

where C_e [mg/L] and Q_e [mg/g] are the MB concentration of solution and the adsorption capacity at equilibrium based on experiments, respectively, while the adsorption affinity, K_e [L/mg], is a calculated value.

To characterize the adsorbents, the specific surface area (by BET method) and pore surface area and pore volume distribution (by *t*-plot method) for all adsorbents were evaluated by N_2 physical adsorption/desorption isotherm at −196 °C using ASAP 2020 (Micromeritics Instrument Corporation, USA). Moreover, the MB adsorption kinetics for each adsorbent was investigated by pseudo-first-order and -second-order kinetic models. Approximately 30 mg of each ground adsorbent was mixed with MB solution at the initial concentration of 200 mg/L for C and NC, 300 mg/L for P, K and Z, and 500 mg/L for NP, NK and NZ, and placed in room at ambient atmosphere. The pseudo-first- and -second-order kinetics parameters were calculated by Eqs. (2) and (3), respectively[13]:

$$\ln \frac{Q_e}{Q_e - Q_t} = k_f t \quad \cdots\cdots (2)$$

where k_f [/h] is the rate constant of pseudo-first-order kinetic model and Q_t is the adsorption capacity at time *t*.

$$\frac{t}{Q_t} = \frac{t}{Q_e} + \frac{1}{k_s Q_e^2} \quad \cdots\cdots (3)$$

where k_s [g/(mg·h)] is the rate constant of pseudo-second-order kinetic model. The elemental composition of carbon, hydrogen and nitrogen for the adsorbents was determined with Perkin Elmer 2400 II (Perkin Elmer Japan, Co., Ltd., Japan). The composition of other components such as oxygen, phosphorus and so on was calculated by difference.

3. Results and Discussion

The MB Langmuir adsorption isotherms are shown in **Fig. 1** and each parameter is summarized in **Table 1**. The activated EFB carbons increased the maximum adsorption capacities up to 143 ~ 256 mg/g from 49 mg/g for the non-activated EFB carbon (**Fig. 1**a). By adding the NaOH pre-washing step, both NP and NZ could achieve higher Q_m than the non-washed adsorbents, but NC and NK showed little improvement in adsorption ability (**Table 1**). Among all the samples, NZ has the highest MB adsorption capacity of 357 mg/g, which is about 1.4 times higher than that of Z. It should be noted that NP, which had the second highest MB adsorption capacity of 303 mg/g, was approximately two times higher than that of P. These results indicate that the NaOH pre-washing treatment for EFB was highly effective for H_3PO_4 activation to improve the adsorption capacity.

The results of BET specific surface area, pore volume and pore average diameter were summarized in **Table 2**. The BET specific surface area of the activated EFB carbons was in the range of 424 ~ 680 m^2/g, which was larger than 293 m^2/g obtained for the carbonized EFB. In the case of the total pore volume, P, K and Z were superior as compared to C, caused by the development of the mesopore volume. $ZnCl_2$ activation developed approximately 2 ~ 3 times greater mesopore surface area and 1.1 ~ 1.5 times larger mesopore volume than those of H_3PO_4 and KOH activation, consequently the MB adsorption amount of Z was higher than that of P and K. The pore structure data would suggest that $ZnCl_2$ activation process involving dehydration was better fitted to EFB because the cell wall was composed of cellulose which might contain abundant hydroxyl groups[14], and then produced

mesopore structure more than H_3PO_4 and KOH activation processes. The NaOH pre-washing samples of NC, NP and NZ had larger specific surface area and total pore volume than C, P and Z, respectively. In the case of mesopore, NP and NZ obtained greater S_{meso} and V_{meso} than P and Z. On the other hand, NC and NK displayed a decrease in mesoporous textural characteristics, compared to C and K. The effect of NaOH steeping on cell wall was reported by Odoch et al.[15] suggesting that cell wall was weakened by NaOH impregnation and then micropores were produced. In this study, NC showed the developed micropores compared to C (**Table 2**). KOH activation also exhibited the effect of increasing micropores similar to H_3PO_4 and $ZnCl_2$ activation, moreover KOH activation could increase the mesopore structure. These results would indicate that both NaOH pre-washing and KOH activation produced micropore relatively more than mesopores in EFB, causing the decrease in MB adsorption capacity from 164 (K) to less than 10 mg/g (NK). For NP and NZ, since the EFB had already produced micropores by NaOH pre-treatment, it would be easy to generate mesopores on EFB surface. In the case of NK, both washing by NaOH (strong base) and impregnation in KOH (strong base as well) for activation would tend to develop micropores and break the cell wall and structure of EFB, therefore EFB was activated more strictly and the cell would be destroyed, hence deteriorating the morphology and pore structures of activated carbon, and decreasing the MB adsorption capacity. **Fig. 2** shows the relationship between textural structure and maximum MB adsorption capacities for each prepared sample. The Q_m and S_{BET} had a linear approximation (**Fig. 2**a), especially S_{meso} would play an important role for the MB adsorption. From the point of pore volume, higher V_{total} led to better MB adsorption capacity. It was found that the maximum MB adsorption capacities increased with increasing the S_{meso}/S_{BET} ratio (**Fig. 2**b) although the opposite relationship was obtained with increasing the S_{micro}/S_{BET} ratio (**Fig. 2**c). In the case of V_{meso}/V_{total} (**Fig. 2**d) and V_{micro}/V_{total} ratio (**Fig. 2**e), the Q_m gave similar relationships as well as **Fig. 2**b and **Fig. 2**c. These observation on the effect of surface area and pore structure implied that not only high S_{BET} and V_{total}, but also high ratio of mesopore and low ratio of micropore of EFB carbon might be important for MB adsorption. These results could be supported by several recent studies that mesoporous materials could effectively adsorb MB compared with microporous adsorbents[16)-19)], even though there were some exceptions[20)].

Fig. 3 shows the results of MB adsorption kinetics. All samples experienced a rapid adsorption at the beginning of 10 hours reaching 90% of saturation, and 24 hours later their adsorption abilities

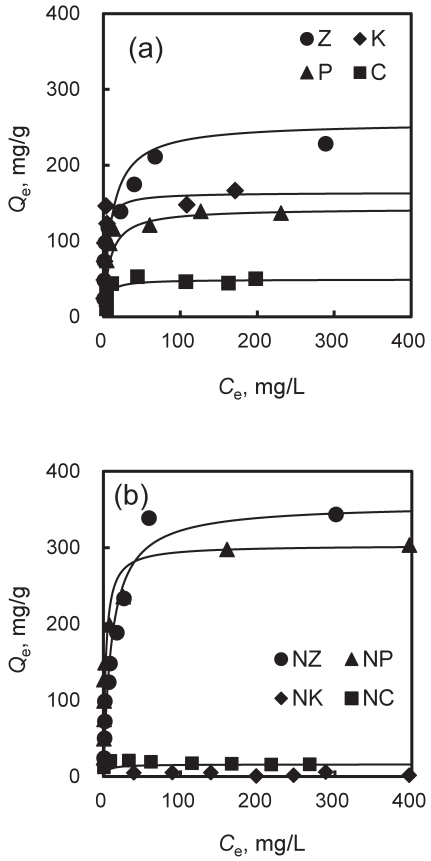

Fig. 1 Langmuir adsorption isotherms of MB onto (a) EFB activated carbons and (b) pre-washed EFB activated carbons.

Table 1 Langmuir isotherm parameters for MB adsorption onto prepared activated carbons.

Sample	Q_m [mg/g]	K_c [L/mg]	R^2
C	49	0.211	0.990
P	143	0.124	0.995
K	164	0.367	0.996
Z	256	0.095	0.995
NC	16	0.185	0.998
NP	303	0.390	0.999
NK	—	—	—
NZ	357	0.092	0.998

Table 2 Textural properties of BET specific and pore surface area, and pore volume of the carbonized/activated EFB.

Sample	S_{BET} [m^2/g]	S_{micro} [m^2/g]	S_{meso} [m^2/g]	S_{micro}/S_{BET} [—]	S_{meso}/S_{BET} [—]	V_{total} [cm^3/g]	V_{micro} [cm^3/g]	V_{meso} [cm^3/g]	V_{micro}/V_{total} [—]	V_{meso}/V_{total} [—]	D_{ave} [nm]
C	293	219	34	0.75	0.12	0.150	0.101	0.040	0.62	0.27	2.05
P	424	204	138	0.48	0.33	0.263	0.092	0.168	0.35	0.64	2.49
K	492	343	73	0.70	0.15	0.296	0.158	0.124	0.53	0.42	2.46
Z	680	273	254	0.40	0.37	0.375	0.122	0.191	0.33	0.51	2.21
NC	332	276	27	0.83	0.08	0.164	0.128	0.028	0.78	0.17	1.98
NP	1090	146	750	0.13	0.69	0.953	0.057	0.836	0.06	0.88	3.50
NK	241	148	51	0.61	0.21	0.157	0.068	0.078	0.43	0.50	2.53
NZ	1270	386	644	0.31	0.51	0.763	0.165	0.504	0.22	0.66	2.42

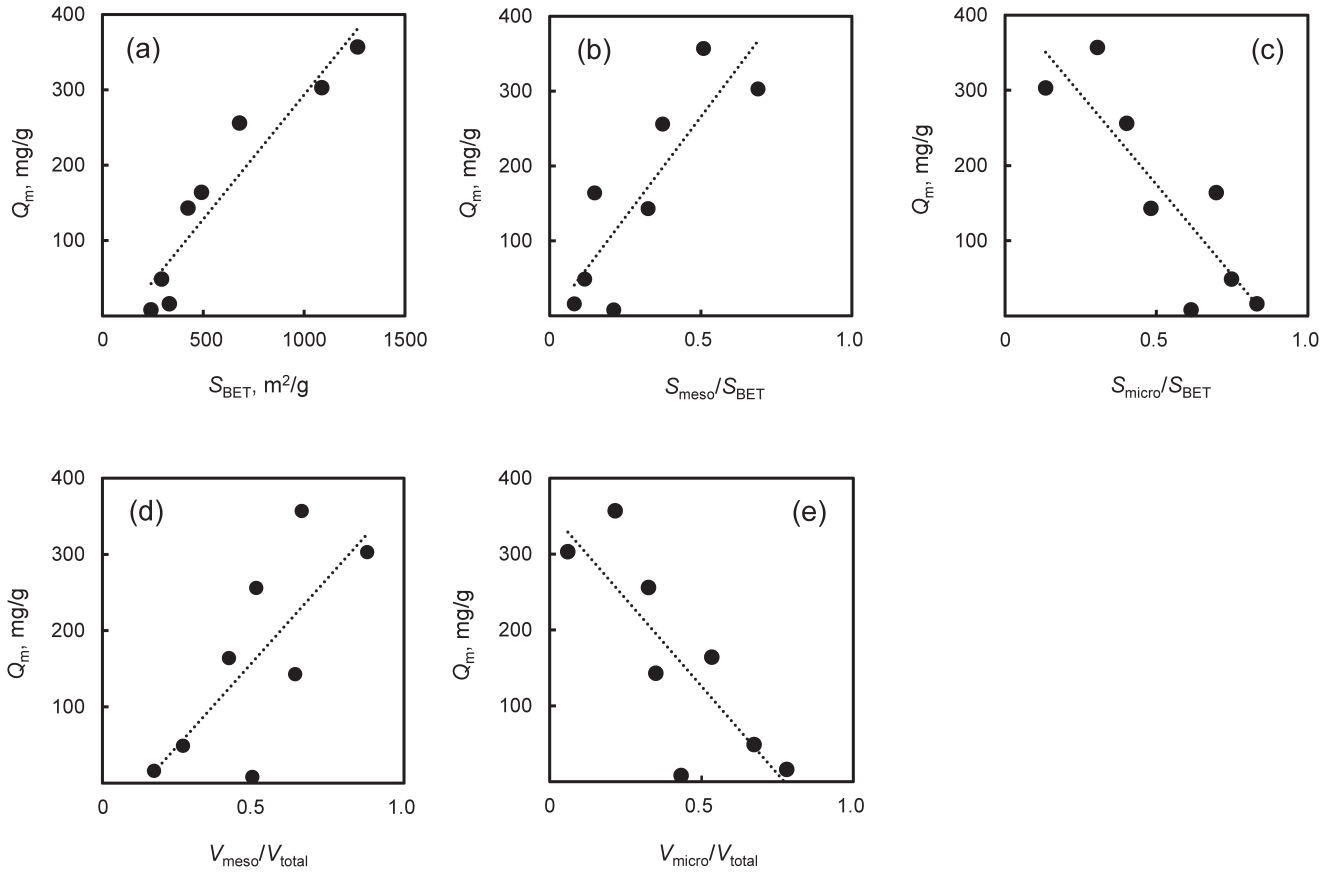

Fig. 2 The effects of (a) S_{BET}, (b) S_{meso}/S_{BET}, (c) S_{micro}/S_{BET}, (d) V_{meso}/V_{total} and (e) V_{micro}/V_{total} on maximum MB adsorption capacities.

were almost in the state of equilibrium. The $Q_{e(cal)}$ calculated from Eqs. (2) and (3), and $Q_{e(exp)}$ averaged from the adsorption capacities (ranging from 18 to 27 hours) were summarized in **Table 3**. Activated EFB carbons were well fitted to pseudo-second-order model, and both $Q_{e(cal)}$ and $Q_{e(exp)}$ were similar. The pseudo-second-order model demonstrates that the MB adsorption onto activated EFB carbons was controlled by diffusion rate. There are no data of C, NC and NK because their adsorption capacities were too small to be calculated. The reason why the adsorption capacity of K and Z was different between the isotherm and kinetics could be attributed to the fact that the kinetic experiment was carried out at initial concentration of 300 mg/L. The isotherm curves were drawn using various concentrations of K (C_0=50 ~ 500 mg/L) and Z (C_0=50 ~ 1000 mg/L), and at low concentration (C_0=300 mg/L) the order of adsorption capacity was K>Z, although that of the maximum adsorption capacity was K<Z. In the case of NP and NZ, the Q_e value was NP>NZ at the initial concentration of 500 mg/L. From the point of adsorption affinities and isotherm curves, K and NP obtained higher K_e than Z and NZ, therefore the adsorption capacities of K and NP were also superior as opposed to those of Z and NZ at low concentration (less than 500 mg/L). However, the EFB activated by $ZnCl_2$ would acquire a relatively high adsorption capacity, so the MB adsorption abilities were not exhausted even at high concentration (higher than 500 mg/L).

The elemental analysis is presented in **Table 4**. The carbon content

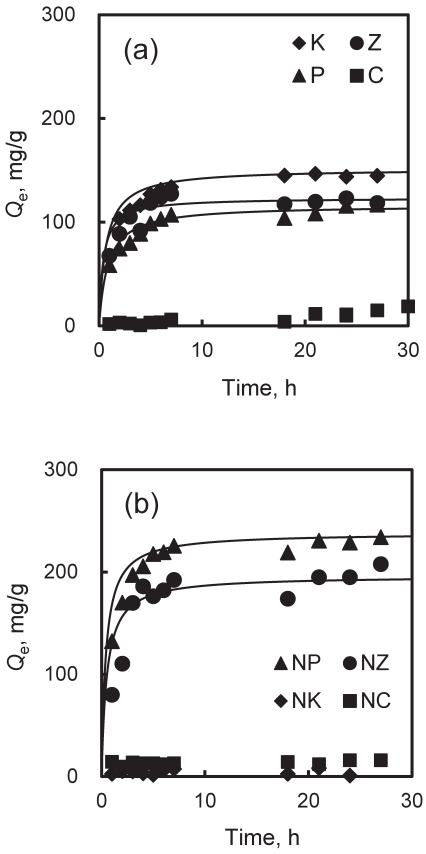

Fig. 3 MB adsorption kinetics onto (a) EFB activated carbons and (b) pre-washed EFB activated carbons.

Table 3 Pseudo-first-order and -second-order kinetic parameters for the carbonized/activated EFB.

Sample	Pseudo-first-order			Pseudo-second-order			$Q_{e(exp)}$ [mg/g]	pH_0	pH_e
	k_f [1/h]	$Q_{e(cal)}$ [mg/g]	R^2	k_s [g/(mg·h)]	$Q_{e(cal)}$ [mg/g]	R^2			
C	—		—	—	—	—	28	6.2	8.5
P	0.37	116	0.921	0.01	116	0.996	109	5.7	5.2
K	0.40	152	0.859	0.01	152	0.999	145	5.7	3.6
Z	0.56	124	0.696	0.02	124	0.997	122	5.7	3.7
NC	—		—	—	—	—	14	6.2	7.8
NP	0.47	238	0.859	0.01	238	0.999	233	5.2	3.4
NK	—		—	—	—	—	5	5.2	4.7
NZ	0.40	196	0.771	0.01	196	0.992	193	5.2	3.7

Table 4 Elemental analysis of the carbonized/activated EFB.

Sample	Carbon [wt%]	Hydrogen [wt%]	Nitrogen [wt%]	Others (oxygen, phosphorus, *etc.*)* [wt%]
C	62.4	1.3	0.8	35.5
P	49.9	0.7	0.7	48.7
K	67.7	1.1	0.7	30.5
Z	70.1	1.0	1.4	27.5
NC	72.4	1.3	1.0	25.3
NP	76.3	1.0	0.6	22.1
NK	78.2	1.7	0.4	19.7
NZ	81.8	1.4	1.0	15.8

* Calculated by difference.

of EFB activated by H_3PO_4 was lower than that of EFB activated by KOH and $ZnCl_2$. This is because the content of elements other than carbon, hydrogen and nitrogen is increased due to the evolution of P=O and P-O originated from PO_4^- group by H_3PO_4 activation[21]. There would be a little difference of hydrogen content among the adsorbents, although Z and NZ contained a slightly more nitrogen content than adsorbents activated by H_3PO_4 or $ZnCl_2$, implying that MB might be adsorbed onto oxygen and nitrogen functional groups on adsorbents, such as hydroxyl, carboxyl and ammonium groups. This phenomenon is supported by the pH values at initial (pH_0) and equilibrium (pH_e) as shown in **Table 3**. In all activated EFB carbons, proton (H^+) was released with decreasing solution pH. However, the extent of mesopore development would largely contribute to MB adsorption than the difference in elemental composition.

4. Conclusion

The EFB activated by H_3PO_4, KOH and $ZnCl_2$ at 600 °C had better MB adsorption ability than the carbonized EFB. Through NaOH pre-washing, the EFB activated by H_3PO_4 and $ZnCl_2$ displayed quite higher maximum MB adsorption capacities (>300 mg/g) than the other samples because NP and NZ developed sufficient BET specific surface area (>1000 m^2/g) and mesopore structures (>500 m^2/g and >0.5 cm^3/g, respectively) compared to P and Z, while NK extinguished the adsorption capacity and surface properties. Based on the relationship between Q_m and textural properties, the amount of MB adsorption would depend on mesopore structure, but not on micropore. The adsorption experiment spent 10 hours to establish the equilibrium state, and the kinetics data were well fitted to pseudo-second-order model.

Acknowledgements

This study was funded in part by the Japan Society for the Promotion of Science (JSPS) under Grant-in-Aid for Scientific Research (C) (No. 26340058) and supported by Tier 1 RUG of Universiti Teknologi Malaysia No. 18H50.

References

1) M. J. Iskandar, A. Baharum, F. H. Anuar and R. Othaman, *Environ. Technol. Innov.* **9** (2018) 169-185.
2) N. Saxena, N. Pal, S. Dey and A. Mandal, *J. Taiwan Inst. Chem. Eng.* **81** (2017) 343-355.
3) C. Y. Keong, *Energy Sources* **27** (2005) 589-596.
4) M. Karina, H. Onggo, A. H. D. Abdullah and A. Syampurwadi, *J. Biol. Sci.* **8** (2008) 101-106.
5) B. Melssen, National Biomass Strategy (2013) ver. 2.0, Agensi Inovasi Malaysia.
6) Z. Ibrahim, A. A. Aziz, R. Ramli, K. Hassan and R. Mamat, Malaysian Palm Oil Board (2017) No. 616, Head of Corporate Implementation and Consultancy Unit.
7) J. Akhtar and A. Idris, *Renew. Energy* **114** (2017) 917-923.
8) K. Y. Foo and B. H. Hameed, *Desalination* **275** (2011) 302-305.
9) S. H. M. Arshad, N. Ngadi, A. A. Aziz, N. S. Amin, M. Jusoh and S. Wong, *J. Energ. Storage* **8** (2016) 257-261.
10) N. B. Osman, N. Shamsuddin and Y. Uemura, *Procedia Eng.* **148** (2016) 758-764.
11) C. H. Ooi, W. K. Cheah, Y. L. Sim, S. Y. Pung and F. Y. Yeoh, *J. Environ. Manage.* **197** (2017) 199-205.
12) M. Hata, Y. Amano, M. Aikawa, M. Machida and F. Imazeki, *TANSO* **2014** [No.261] 2-7 [in Japanese].
13) S. Kilpimaa, H. Runtti, T. Kangas, U. Lassi and T. Kuokkanen, *J. Ind. Eng. Chem.* **21** (2015) 1354-1364.
14) I. Ozdemir, M. Şahin, R. Orhan and M. Erdem, *Fuel Process. Technol.* **125** (2014) 200-206.
15) M. Odoch, E. M. Buys and J. R. N. Taylor, *Food Chem.* **228** (2017) 338-347.
16) F. Marrakchi, M. J. Ahmed, W. A. Khanday, M. Asif and B. H. Hameed, *Int. J. Biol. Macromol.* **98** (2017) 233-239.
17) X. Zhang, L. Cheng, X. Wu, Y. Tang and Y. Wu, *J. Environ. Sci.* **33** (2015) 97-105.
18) E. I. EI-Shafey, S. N. F. Ali, S. Al-Busafi and H. A. J. Al-Lawati, *J. Environ. Chem. Eng.* **4** (2016) 2713-2724.
19) A. Murray and B. Örmeci, *J. Environ. Sci.* **66** (2018) 310-317.
20) A. A. Spagnoil, D. D. Giannakoudakis and S. Bashkova, *J. Mol. Liq.* **229** (2017) 465-471.
21) X. Liu, C. He, X. Yu, Y. Bai, L. Ye, B. Wang and L. Zhang, *Powder Technol.* **326** (2018) 181-189.